agronomy

MDPI

Article

Investigating the Spatial Structure of Soil Hydraulic Properties in a Long-Term Field Experiment Using the BEST Methodology

Stefano Popolizio [1], Emanuele Barca [2,*], Mirko Castellini [3], Francesco F. Montesano [1] and Anna Maria Stellacci [1]

[1] Department of Soil, Plant and Food Sciences, University of Bari Aldo Moro, Via Amendola 165/A, 70126 Bari, Italy
[2] Water Research Institute (IRSA)—National Research Council (CNR), Viale Francesco de Blasio 5, 70132 Bari, Italy
[3] Council for Agricultural Research and Economics—Research Center for Agriculture and Environment (CREA-AA), Via C. Ulpiani 5, 70125 Bari, Italy
* Correspondence: emanuele.barca@irsa.cnr.it

Abstract: Understanding the spatial structure of soil properties at field scale and introducing this information into appropriate data analysis methods can help in detecting the effects of different soil management practices and in supporting precision agriculture applications. The objectives of this study were: (i) assessing the spatial structure of soil physical and hydraulic properties in a long-term field experiment; (ii) defining a set of spatial indicators for gaining an integrated view of the studied system. In seventy-two georeferenced locations, soil bulk density (*BD*), initial volumetric soil water content (θ_i) and cumulative infiltration curve as function of the time ($I(t)$) were measured. The soil water retention curve ($\theta(h)$) and the hydraulic conductivity function ($K(h)$) were then estimated using the Beerkan Estimation of Soil Transfer parameters (BEST) methodology. The volumetric soil water contents at soil matrix ($h = -10$ cm), field capacity ($h = -100$ cm) and wilting point ($h = -15{,}300$ cm) were considered. In addition, a set of capacitive indicators—plant available water capacity (*PAWCe*), soil macroporosity (*PMACe*), air capacity (*ACe*) and relative field capacity (*RFCe*)—were computed. The data were first analyzed for overall spatial dependence and then processed through variography for structural analysis and subsequent spatial interpolation. Cross-correlation analysis allowed for assessing the spatial relationships between selected physical and hydraulic properties. On average, optimal soil physical quality conditions were recorded; only *PMACe* values were indicative of non-optimal conditions, whereas mean values of all the other indicators (*BD*, *Ks*, *PAWCe*, *ACe*, *RFCe*) fell within optimal ranges. The exponential model was found to be the best function to describe the spatial variability of all the considered variables, except *ACe*. A good spatial dependence was found for most of the investigated variables and only *BD*, *ACe* and *Ks* showed a moderate autocorrelation. *Ks* was confirmed to be characterized by a relatively high spatial variability, and thus, to require a more intensive spatial sampling. An inverse spatial cross-correlation was observed between *BD* and *Ks* up to a distance of 10 m; significant cross-correlations were also recorded between *Ks* and *PMACe* and *ACe*. This result seems to suggest the possibility to use these soil physical quality indicators as covariates in predictive multivariate approaches.

Keywords: beerkan estimation of soil transfer parameters (BEST) methodology; saturated hydraulic conductivity; soil physical quality; capacitive indicators; spatial autocorrelation; nugget-to-sill ratio; exponential model; cross-correlation

Citation: Popolizio, S.; Barca, E.; Castellini, M.; Montesano, F.F.; Stellacci, A.M. Investigating the Spatial Structure of Soil Hydraulic Properties in a Long-Term Field Experiment Using the BEST Methodology. *Agronomy* **2022**, *12*, 2873. https://doi.org/10.3390/agronomy12112873

Academic Editors: Jinman Wang and Long Guo

Received: 29 September 2022
Accepted: 15 November 2022
Published: 16 November 2022

1. Introduction

A clear understanding of the impact of agronomic techniques on soil quality and crop productivity is of foremost importance for the sustainable management of cropping systems and for providing proper answers to challenges posed by climate change. Soil tillage

practices are known to greatly affect soil status and quality [1,2] and its ability to capture and store precipitation or irrigation water [3]. The direct action of tillage management on soil physical properties modifies air-water capacity relationships. This in turn affects soil organic matter dynamics and turnover, carbon storage and CO_2 emissions, nutrient cycling and water resources conservation [1,2,4,5].

Modifications induced by tillage practices on soil physical and hydraulic properties are not always easy to detect, and field studies have often provided contrasting results [3]. The presence of unstable conditions, when investigations are carried out in the short- and medium-term period, and also the spatial variability of the soil properties over the field experimental area may cause difficulty in discerning the effects. Spatial heterogeneity is suggested as a primary source of error [6]. When spatial variability occurs at a scale smaller than the block (and plot) size, the effect of experimental treatments on the response of primary variables may be confounded [7–9]. Several studies have reported that neglecting the spatial dependence can cause misinterpretation errors, and consequently, improper management decisions [10,11].

In order to assess the spatial structure of the investigated variables, specific approaches for data sampling and analysis have to be undertaken. At first instance, a more intensive sampling is required in comparison to traditional approaches. A number of samples ranging from 50 to 100 is appropriate for accurate spatial analysis [12–14]. Sample sizes below 50 units do not meet the basic assumption for the application of spatial analysis [15,16].

In addition, multiple, or repeated, measurements performed over the same experimental unit/plot may give rise to correlations among observations and/or residuals that need to be appropriately considered in statistical analysis [7]. In this specific case, not properly accounting for residual autocorrelation over space may cause erroneous conclusions about treatment significance [10]. Modeling the variance-covariance matrix of the residuals and incorporating this information into linear mixed effects models (LMMs) may represent a rigorous approach alternative to classical analysis of variance and standard linear models. The information about the spatial structure of a variable of interest can support farmers in delineating homogeneous areas for promoting the application of precision agriculture strategies.

The need for denser sampling in spatial studies is, however, hindered by the characteristics of conventional methods for determination of soil physical and hydraulic properties, since these methods are expensive and time consuming, and often require high technical skills. Simple, quick and accurate methodologies are envisaged and desirable [17]. A simple and rapid field method, initially developed by Haverkamp et al. [18], allowed for the simultaneous characterization of both hydraulic conductivity function and water retention curve. Lassabatère et al. [19] developed the "Beerkan Estimation of Soil Transfer parameters (BEST)" procedure in order to simplify soil hydraulic characterization [20]. The method can be conveniently applied for performing intensive samplings with a less demanding experimental effort [21], thus dealing with the requirements of spatial analysis.

Another open issue in the field of spatial analysis is that of selecting a suitable number of effective indicators, and above all, to learn how to interpret them in an integrated way. In the past, several efforts have been directed toward reaching this aim, and not always with satisfying results [22,23]. Today, it is possible to collect a large amount of literature regarding a number of old and newly introduced indicators without any attempt at presenting an integrated reading of the results provided. More specifically, the Moran index has a long-dated history, during which the method by which to use it and the related interpretation of the results have significantly improved [24]. In addition to the Moran index, even the nugget-to-sill ratio [25–27] has evolved to include the range and the model itself within the computation [27]. The cross-correlogram is a very powerful tool to quantitatively compare different spatial maps, thus reducing the subjectivity of visual inspection [28,29]. However, this index is often neglected in spatial analysis studies due to the difficulty in computing and interpreting the results. After the refinements of the concepts underlying those indicators, the revision of the definitions and the overcoming of misconceptions, the

issue of misinterpretation or contradiction among results provided by different indicators has become much rarer. Therefore, an integrated reading of the outcomes of many indices together is not only possible, but desirable. In the present study, a set of indicators were applied to a group of variables with different degrees of spatial correlation in order to provide a systematic and integrated approach and "read between the lines" of the specific spatial features of different variables.

The general objective of this study was to assess the spatial structure of soil physical and hydraulic properties at a long-term field experimental site. Secondly, a set of spatial indicators for gaining an integrated view of the studied system were suggested and used. The BEST-procedure was adopted for the soil hydraulic characterization. The data, collected in georeferenced locations, were first analyzed for overall spatial dependence and then processed through variography for structural analysis and subsequent spatial interpolation. The quantitative assessment of the spatial relationships between selected physical and hydraulic properties was finally achieved using cross-correlation analysis. This study will also represent a preliminary step toward the inclusion of the information on the spatial structure of the investigated variables into linear mixed effects models considering residual autocorrelation. Moreover, information about spatial structure can support farmers in delineating management zones for fostering the application of precision agriculture strategies.

2. Materials and Methods

2.1. Study Area and Experimental Trial

The field experiment was performed in the autumn of 2021 at the Council for Agricultural Research and Economics (CREA-AA) in Southern Italy (41°27′03″ N, 15°30′06″ E). The climate is classified as *accentuated thermomediterranean* [30]. Long-term annual average rainfall is 550 mm and it is mainly concentrated in the winter period [9]. The soil is clay of alluvial origin classified as fine, mesic, Typic Chromoxerert [31].

Data were collected within a long-term field experiment, started in 2002, aimed at investigating the effects of two soil management strategies (minimum tillage, MT, and no-tillage, NT) on durum wheat (*Triticum turgidum* subsp. *durum* Desf.). The experimental design was a randomized complete block design (RCBD) with three replicates and unit plot sizes of 500 m^2. Further details on the experimental trial and plot management are reported in Castellini et al. [32] and Stellacci et al. [5].

Measurements of soil physical and hydraulic properties were carried out in seventy-two geo-referenced locations. The number of observations was defined to gain a minimum number of pairs for each distance class in order to assess spatial structures underlying the physical process taking place in the study area [14].

2.2. Laboratory and Field Measurements

The Beerkan Estimation of Soil Transfer Parameter (BEST) methodology by Lassabatère et al. [19] was applied for each of the selected seventy-two sampling locations. In particular, at each sampling point, the soil bulk density (*BD*), the initial volumetric soil water content (θ_i) and the cumulative infiltration curve as function of the time ($I(t)$) were determined. Then, the soil water retention curve and the hydraulic conductivity function ($\theta(h)$ and $K(h)$ relationships, respectively) were estimated using the BEST methodology. The values of the volumetric soil water content corresponding to specific reference values of the matrix potential, i.e., at soil matrix, θ_{10} ($h = -10$ cm), at field capacity, θ_{100} ($h = -100$ cm) and at wilting point, θ_{15300} ($h = -15{,}300$ cm), were taken into account and analyzed to investigate the spatial variation of soil physical properties. In addition, starting from the estimated soil water retention curve, a set of four capacitive indicators accounting for the proportion between water and air into the soil was computed. These indicators were: plant available water capacity (*PAWCe*), soil macroporosity index (*PMACe*), air capacity (*ACe*) and relative field capacity (*RFCe*) [33]. More information on these indicators is reported in the following sections.

In detail, an infiltration experiment was carried out at each sampling point using a metal ring (15 cm inner diameter) and the cumulative infiltration as a function of the time ($I(t)$) was measured. Fifteen water volumes of 200 mL each were poured from a height of about 3 cm and the BEST-steady algorithm [34] was applied to estimate the soil water retention curve and the hydraulic conductivity function ($\theta(h)$ and $K(h)$). Undisturbed soil cores (0.10 m in height by 0.05 m in diameter) were collected in each sampling point at a 0 to 0.10 m depth close to the ring to quantify the soil water content at the beginning of infiltration experiments, θ_i, and the soil dry bulk density (*BD*). Saturated soil water content, θ_s, was estimated from *BD* assuming a particle density of 2.65 g cm^{-3}. Disturbed soil samples were also collected at each sampling point to assess the mean particle size distribution (*PSD*) at 0–0.10 m depth. After checking that quasi-steady flow conditions were always reached, *BD*, θ_i, *PSD* and $I(t)$ were used to run BEST-steady. Therefore, although the average values of the input variables are usually used for running BEST, in this investigation, only the mean *PSD* was used, while the single geo-referenced observations of *BD*, θ_i and $I(t)$ were considered.

2.3. Soil Physical Indicators

The soil saturated hydraulic conductivity (*Ks*) indicates the soil water infiltration capacity and is a key property affecting soil water storage, and the transport of water and solutes in the soil [35,36]. Optimal *Ks* values for agriculture soils, ranging within 0.005–0.05 mm s^{-1}, favor a rapid infiltration and redistribution of plant available water [35,36]. Dry bulk density (*BD*) is an indicator of soil quality, correlated with soil compaction, related to soil porosity and moisture content. It is also related to thermal properties (soil volumetric heat capacity, thermal conductivity), in this way affecting chemical and biological variables. Optimal *BD* values range in an interval between 0.9–1.2 g cm^{-3}. *BD* and *Ks* have been widely used to explore the impact of soil management from the point of view of environmental sustainability (among others, Cavalcante et al. [37]), and have been recently included in specific protocols for the assessment of sustainable soil management [38].

Plant available water capacity (*PAWC*) (cm^3 cm^{-3}) is computed as the difference between the water contents at field capacity (at $h = -100$ cm) and at permanent wilting point (at $h = -15{,}300$ cm) [32], and thus, represents the water available for crop growth. For the present investigation, the following *PAWC* limits were considered [36]: $PAWC \geq 0.20$ ideal; $0.15 < PAWC < 0.20$ good; $0.10 < PAWC < 0.15$ limited; $PAWC < 0.10$ poor. Air capacity (*AC*) (cm^3 cm^{-3}) is computed as the difference between the water contents at saturation and at field capacity; providing information about the soil ability to store and transmit air [36]. Optimal *AC* values for clay soil fall in the interval 0.10–0.26 cm^3 cm^{-3}, while higher or lower values indicate poor soil aeration conditions [32,33]. The relative field capacity (*RFC*) was computed as the ratio between the water contents at field capacity and at water saturation [36]. Optimal values for *RFC* range within the interval 0.6–0.7; lower or higher values indicate "water limited" or "aeration limited" conditions, respectively [36]. Macroporosity (*PMAC*) (cm^3 cm^{-3}) gives the volume of large (macro) pores (i.e., >0.3 mm equivalent pore diameter), which indirectly indicates the soil's ability to quickly drain excess water and facilitate root proliferation. $PMAC \geq 0.05$–0.10 cm^3 cm^{-3} indicates optimal conditions, while $PMAC \leq 0.04$ cm^3 cm^{-3} indicates soil compaction [39–41].

The subscript *e* (i.e., *PAWCe*, *ACe*, *RFCe*, *PMACe*) is used for indicating variables estimated by BEST. Since indicators of soil quality were both estimated by BEST and directly measured (*BD* and *Ks*), they assume a different meaning. Consequently, capacitive indicators (i.e., *PAWCe*, *ACe*, etc.) could provide evidence of better or worse relative soil quality, according to the different soil use or to the relative distance within the plot.

2.4. Statistical Methods

2.4.1. Exploratory and Correlation Data Analysis

Basic statistics were computed for the investigated variables: *BD*, *ACe*, *PMACe*, *PAWCe*, *RFCe*, *Ks*, θ_i, θ_{10}, θ_{100} and θ_{15300}. Finally, the hypothesis of normality was checked using Shapiro-Wilk test.

Pearson correlation coefficients were computed in order to investigate the relationships among studied variables. Moreover, the assessment of the overall spatial correlation of the considered variables was performed by means of Moran statistics [42,43]. Details regarding the Moran I index can be found in the following papers [32,42,43].

2.4.2. Geostatistical Analysis

The spatial variability of a variable can be assessed by means of the geostatistical analysis with the aim of predicting variable values at unvisited locations and producing maps. The main stages of geostatistical analysis concern structural analysis (variography), weight assessment and, finally, interpolation (kriging).

Variography

The experimental variogram and the variogram model are two different functions used to describe the features of geo-referenced data. The experimental variogram is a discrete function and represents the half of the average squared difference between points separated by the distance h (lag). The variogram model is a mathematical model parametric, a continuous and conditionally negative definite [22] (Figure 1). The variogram model is derived from the experimental variogram by means of a procedure called model fitting. In Figure 1, some examples of theoretical variogram models are reported.

Model	Variogram	Parameters Restriction
Matérn	$\gamma(h) = \sigma^2[1 - (\alpha h)^{\nu}\mathcal{K}_{\nu}(\alpha h)]$	$\nu > 0$
Exponential	$\gamma(h) = \sigma^2(1 - exp(-h/\alpha))$	
Gaussian	$\gamma(h) = \sigma^2(1 - exp(-h/\alpha)^2)$	
Spherical	$\gamma(h) = \sigma^2\left[(1 - h/\alpha)^2 + (1 + h/2\alpha)\right]$	
Power	$\gamma(h) = \sigma^2(h/\alpha)^a$	$0 < a \leq 2$

(**a**)

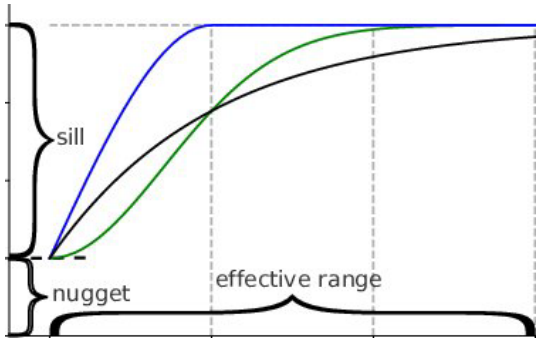

(**b**)

Figure 1. Examples of parametric families of theoretical models for experimental variograms fitting (**a**); comparison of spherical (upper function), Gaussian (intermediate function) and exponential (lower function) models (**b**). Modified from Mälicke et al. [44].

The parameters of the variogram model are the partial sill (σ^2), indicating the structured component of the variance, the nugget, indicating the random uncorrelated component, and the range (α). The range is defined as the distance beyond which the spatial correlation becomes negligible (Figure 1). For asymptotic models, such as Gaussian and exponential, the true range is replaced by the effective (or practical) range that is defined as the distance at which the semivariance value achieves 95% of the sill [45,46].

In this study, variogram models were used to model the experimental variograms of the investigated physical and hydraulic variables. The goodness-of-fit was evaluated through the leave-one-out cross-validation and Pearson correlation coefficients (r) between predicted and observed data were computed [22].

Spatial Interpolation

Ordinary kriging (*OK*) was selected as well suited to interpolate the investigated variables. OK is a univariate predictor in which the unknown value $z(x_0)$ of a given realization of $Z(x_0)$ is predicted from the known values $z(x_i)$ $i = 1, 2, \ldots, N$, at the support points x_i. The OK predictor is expressed as described in the following papers [26,29,47].

2.4.3. Cross-Correlation

Cross-correlations were computed for comparing the maps of the interpolated values of the studied variables. The cross-correlation is effective in highlighting the strength and the extent of the spatial correlation between a couple of variables [28,29,48]. The analytical formulation is the following:

$$\rho_{A,\,B}(h) = \frac{E\left[z_{i,jA}, z_{i',j'B}\right] - m_A \cdot m_B}{s_A \cdot s_B} \quad (1)$$

where $z_{i,jA}$ and $z_{i',j'B}$ represent the values at locations $(i - i\prime)$ and $(j - j\prime)$ of the two maps separated by the h distance, respectively; $h = \sqrt{(i - i\prime)^2 + (j - j\prime)^2}$ represents the distance between the two locations, E denotes the mathematical expectation, m_A and m_B represent the populations means and s_A and s_B represent the populations standard deviations. If patterns are completely similar, apart from a constant, $\rho_{A,\,B}(1)$ should be equal to 1. To estimate $\rho_{A,\,B}(h)$ from the available data the following equation can be used:

$$r_{A,\,B}(h) = \frac{\sum_{i,j=1}^{N(h)} z_{i,jA}, z_{i',j'B} - \hat{m}_A \cdot \hat{m}_B}{\hat{s}_A \cdot \hat{s}_B} \quad (2)$$

To compute $r_{A,\,B}(h)$, the procedure is as follows: from both maps, all the couples whose locations are separated by the distance h are collected. Indices $\hat{m}_A$ and $\hat{m}_B$ and $\hat{s}_A$ and $\hat{s}_B$ represent the mean and the standard deviation of mapped $z_{i,jA}$ and $z_{i',j'B}$, respectively. *N(h)* is the total number of these pairs.

The cross-correlation coefficients obtained at specified lag distances (0 m, 5 m, 10 m, 15 m, 20 m) were reported in order to provide quantitative information on the spatial relationships of soil physical and hydrological variables under study.

3. Results

3.1. Exploratory Data Analysis

The basic statistics highlighted a departure from the normal distribution of all the variables under study, excluding bulk density (*BD*), according to the Shapiro-Wilk test. Nonetheless, as shown in Table 1, skewness was almost always smaller than 1, indicating that distributions of considered variables were nearly symmetrical; therefore, values were not transformed into Gaussian.

Table 1. Summary statistics for the variables under study.

Variable	Unit	Mean	St.Dev	Median	Min	Max	Skewness	Kurtosis
Ks	mm s^{-1}	0.043	0.055	0.016	0.001	0.270	1.864	3.630
θ_i	cm^3 cm^{-3}	0.347	0.029	0.351	0.247	0.399	−1.548	2.989
θ_{10}	cm^3 cm^{-3}	0.599	0.028	0.606	0.526	0.65	−0.586	−0.357
θ_{100}	cm^3 cm^{-3}	0.426	0.041	0.434	0.33	0.487	−0.621	−0.655
θ_{15300}	cm^3 cm^{-3}	0.147	0.016	0.151	0.112	0.174	−0.440	−0.745
BD	g cm^{-3}	1.008	0.051	1.002	0.904	1.129	0.286	−0.681
PMACe	cm^3 cm^{-3}	0.020	0.017	0.012	0.005	0.092	1.811	3.211
ACe	cm^3 cm^{-3}	0.193	0.034	0.183	0.141	0.291	0.817	−0.277
PAWCe	cm^3 cm^{-3}	0.279	0.025	0.285	0.218	0.315	−0.706	−0.593
RFCe	-	0.687	0.057	0.699	0.537	0.761	−0.823	−0.463

3.2. Soil Physical Indicators

Measured values of physical and hydraulic variables were compared with the optimal ranges reported in the literature, as summarized in Section 2.3. Overall, observed values showed good average results as only *PMACe* values were indicative of non-optimal conditions, whereas mean values of all the other indicators (*BD*, *Ks*, *PAWCe*, *ACe*, *RFCe*) fell within optimal ranges (Table 1).

In more detail, *BD* showed optimal soil density with the entire range of variation of the measurements (0.904–1.129 g cm^{-3}) falling in the interval 0.9–1.2 g cm^{-3} (Table 1). These results were also in agreement with those provided by *ACe* that always showed values in the interval 0.10–0.26 cm^3 cm^{-3}, except for two observations (0.2718 and 0.2917 cm^3 cm^{-3}). Regarding *RFCe*, although the values recorded at some locations were outside the optimal range (0.6–0.7), these observations were very close to the critical limits with average values of 0.73 and 0.58, respectively; in addition, only two values were lower than 0.55 and only four values were greater than 0.75. Optimal conditions were also recorded for *PAWCe* at all the sampling locations with observed values always greater than 0.20 cm^3 cm^{-3}; in particular, about 80% of the observations showed *PAWCe* values greater than 0.25 cm^3 cm^{-3}. In these locations, as expected, the lowest values of *PMACe* were also recorded with values lower than 0.04 cm^3 cm^{-3}. Finally, good hydrodynamic soil properties were observed. The average value of *Ks* (0.043 mm s^{-1}) fell within the limits defined in the literature [35] and the observed values lower than the critical limit (<0.005 mm s^{-1}) were quite close to this critical threshold, with only three locations showing values of saturated hydraulic conductivity smaller than 0.002 mm s^{-1}.

3.3. Correlation and Preliminary Spatial Analysis

Interesting relationships were observed among the soil variables (Table 2). Significant correlations were observed between *Ks* and *PMACe* and *ACe* (r = 0.81 and 0.80, $p < 0.0001$). A negative correlation was instead observed between *Ks* and the two capacitive indicators *RFCe* and *PAWCe* (−0.816, −0.764). Strong positive correlations were found between *RFCe* with *PAWCe*, θ_{100} and θ_{15300} (r = 0.937, 0.908, 0.855, $p < 0.0001$), while negative correlations were found with *Ks*, *PMACe* and *ACe* (r = −0.81, −0.99, −0.97, $p < 0.0001$). *PAWCe* was strongly negatively related to *PMACe* and *ACe* (r = −0.896, −0.85, $p < 0.0001$), while there was a high positive correlation with θ_{10}, θ_{100}, θ_{15300} and *RFCe* (r = 0.87, 0.99, 0.976, 0.937, $p < 0.0001$). Finally, *BD* showed significant inverse correlations with values of volumetric soil water content at −10 cm, −100 cm and −15,300 cm, namely −0.84, −0.6, −0.68, and at the beginning of the experiment (θ_i), of −0.52.

Table 2. Pearson's correlation matrix for the variables under study.

Variable	*Ks*	θ_i	θ_{10}	θ_{100}	θ_{15300}	*BD*	*PMACe*	*ACe*	*PAWCe*	*RFCe*
Ks	1									
θ_i	0.015	1								
θ_{10}	−0.545	0.522	1							
θ_{100}	−0.752	0.447	0.902	1						
θ_{15300}	−0.698	0.478	0.945	0.990	1					
BD	0.187	−0.523	−0.839	−0.603	−0.683	1				
PMACe	0.812	−0.273	−0.592	−0.860	−0.798	0.168	1			
ACe	0.804	−0.235	−0.523	−0.810	−0.743	0.083	0.992	1		
PAWCe	−0.764	0.447	0.869	0.995	0.976	−0.551	−0.895	−0.850	1	
RFCe	−0.816	0.317	0.669	0.909	0.855	−0.270	−0.990	−0.972	0.937	1

Moran index, indicating the overall spatial dependence, ranged from values of 0.16 ($p = 0.04$) and 0.196 ($p = 0.023$) for *BD* and *Ks*, indicating a poor spatial correlation, to values of 0.4063, 0.4329, 0.4360, 0.4364 and 0.480 (with p values < 0.001), for θ_{10}, *PAWCe*, θ_{100}, θ_{15300}, θ_i, respectively, indicating a good spatial dependence.

3.4. Variography and Spatial Interpolation

Theoretical nested models, consisting of a nugget effect and a spatial covariance function, were used to model the experimental variograms of the investigated variables. The test for the anisotropy was performed and it was found not significant; then, isotropic models were selected for all the studied variables. Results, reported in Table 3, showed that the exponential model was found to be the best theoretical function according to the considered error metrics, being chosen for all the variables except air capacity (*ACe*). The nugget-to-sill ratio was computed to assess the spatial structure of the variables [25], with ratios lower than 25% indicating strong spatial dependence, ratios between 25 and 75% indicating moderate spatial dependence and ratios greater than 75% indicating weak spatial dependence. The analysis of the observed values of nugget-to-sill ratio indicated a significant spatial structure for most of the variables investigated with values lower or close to 25% (Table 3). Greater values were recorded for *BD* (0.46) and *Ks* (0.4725), confirming the results of the Moran I index that showed a poor overall spatial structure for these variables, and for *ACe* (0.45). The lowest values were recorded for volumetric soil water content at the beginning of the experiment (θ_i) and of the soil matrix (θ_{10}).

Table 3. Model selected, variogram parameters, nugget-to-sill ratio and cross-validation outcomes.

	Ks	$\boldsymbol{\theta_i}$	$\boldsymbol{\theta_{10}}$	$\boldsymbol{\theta_{100}}$	$\boldsymbol{\theta_{15300}}$	***BD***	***PMACe***	***ACe***	***PAWCe***	***RFCe***
Nugget	0.00228	0	5.24×10^{-05}	0.00039	3.7×10^{-05}	0.0013	0.00021	0.00080	0.00018	0.0016
Partial sill	0.00254	0.0014	0.0009	0.0018	2.8×10^{-04}	0.0015	0.00056	0.00096	0.00074	0.009
Nugget-to-sill ratio	0.4725	0	0.055	0.17	0.1156	0.46	0.27	0.45	0.20	0.15
Range	107.547	18	11.83	19.01	14.34	7.73	9.77	34.74	23.29	113.97
Model	Exp	Exp	Exp	Exp	Exp	Exp	Exp	Gau	Exp	Exp
Pred. vs. obs. (r)	0.3841	0.7	0.58	0.62	0.62	0.23	0.54	0.54	0.62	0.57

Cross-validation outcomes showed that the correlation between predicted and observed values (pred. vs. obs.) was lower than 0.6 for *Ks*, *BD*, *PMACe* and *ACe*. All the other variables showed a pred. vs. obs. correlation larger than or closer to (*RFCe* and θ_{10}) 0.6 and were then sufficient. The best variable was θ_i, with a correlation between predicted and observed values equal to 0.7 (Table 3).

From the visual inspection of the resulting maps (Figures 2 and 3), a significant spatial structure emerged for all investigated variables. Initial volumetric soil water content (θ_i) showed a single zone with lower values in the southern part of the map and the larger values mainly located in the upper left portion. The *BD* map showed a specular behavior with respect to the previous variable, and thus, with the larger values located in the southern right zone. The maps of estimated volumetric soil water contents (θ_{10}, θ_{100} and θ_{15300}) displayed similar characteristics each other and with θ_i, with lower values on the southern right part and higher values on the top of the maps; in addition, another zone with lower values was observed on the middle left part of the three maps.

As expected, maps of *PAWCe* and *RFCe* shared some characteristics with θ_{100} and θ_{15300}, being derived from these variables (Figure 3). *PMACe* and *ACe* were similar to each other and mirrored *PAWCe* and *RFCe*, confirming the results of the correlation analysis. In the middle longitudinal region, *Ks* map recalled the behavior observed for *PMACe* and *Ace*, and, consequently, of the estimated volumetric soil water content maps. Furthermore, there was also observed a similarity with the values located in the right southern and the middle left portions of the maps.

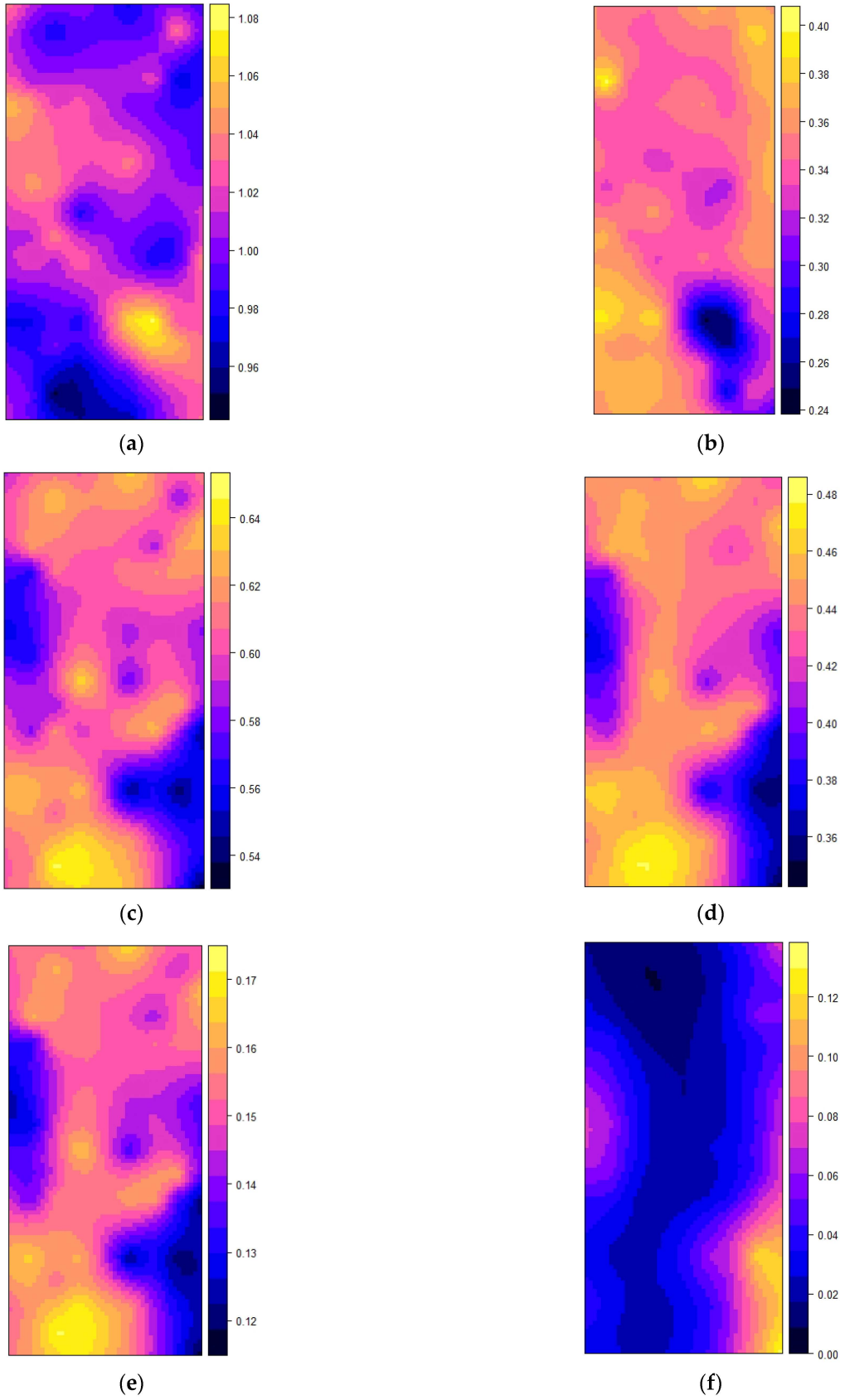

Figure 2. Maps of the interpolated values of *BD* (**a**), θ_i (**b**), θ_{10} (**c**), θ_{100} (**d**), $\theta_{15,300}$ (**e**), *Ks* (**f**).

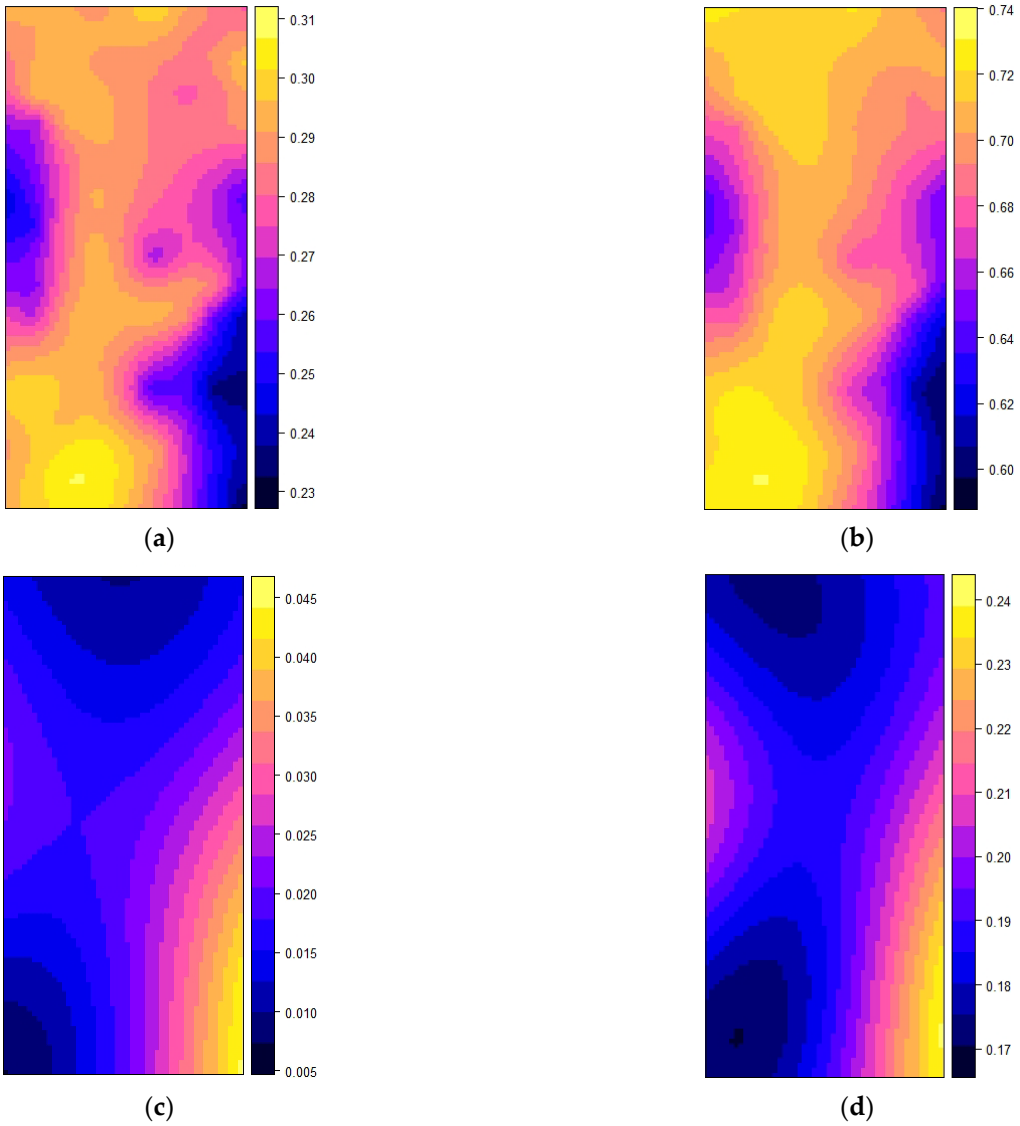

Figure 3. Maps of the interpolated values of *PAWCe* (**a**), *RFCe* (**b**), *PMACe* (**c**), *ACe* (**d**).

To enhance these results, some variables were selected to check direct or inverse spatial behavior through cross-correlation procedures (*BD*, *Ks*, *PMACe* and *ACe*). Table 4 highlights an inverse cross-correlation between *BD* and *Ks* up to a distance of 10 m; this result was coherent with the spatial structure of *BD*, for which the range was lower than 10 m (7.7 m; Table 3). For this reason, all values related to distances larger than that length should be considered unreliable. The sign of the relationship between the two variables derives from the Pearson linear correlation reported in Table 2. Significant spatial cross-correlations were also recorded between *Ks* and the two capacitive indicators *PMACe* and *ACe*. Even for these last variables, the range of correlation was around 10 m, confirming once more the results displayed in Table 3. The strong cross-correlations observed were expected after visual inspection of the reported maps (Figures 2 and 3). Finally, as anticipated, a strong cross-correlation in the same spatial range was found for the two capacitive indicators, *PMACe* and *ACe* (Table 4).

Table 4. Cross-correlation coefficients computed at different lags (0, 5, 10, 15, 20 m) between *BD*, *Ks* and the two capacitive indicators *PMACe* and *ACe*.

	0 m	5 m	10 m	15 m	20 m
BD vs. *Ks*	−0.2800	−0.1774	−0.1066	−0.0482	0.0263
PMACe vs. *Ks*	0.6578	0.3649	0.1952	0.1033	0.0379
ACe vs. *Ks*	0.6311	0.3504	0.1881	0.0995	0.0322
PMACe vs. *ACe*	0.7190	0.4041	0.2216	0.1276	0.0544

4. Discussion

The presence of spatial autocorrelation of soil variables in the experimental field can represent a major factor to be considered for revealing the impact of agronomic management on soil physical and hydraulic properties. This study provided a practical methodology for the assessment of the existence of a spatial structure of the variables investigated. These results will also represent a preliminary step for the inclusion of information regarding linear mixed effects models considering residual autocorrelation.

The assessment of soil physical and hydraulic status carried out with reference to the scientific literature showed that near optimal conditions were recorded in the experimental site; only *PMACe* average values were indicative of non-optimal conditions, whereas mean values of all the other indicators (*BD*, *Ks*, *PAWCe*, *ACe*, *RFCe*) fell within optimal ranges. However, we would like to point out that soil physical quality evaluation must be considered as indicative for the variables estimated from BEST (i.e., plant available water, air capacity) and closer to physical reality for the variables directly measured (i.e., bulk density and saturated hydraulic conductivity). In this sense, the literature references were used as benchmarks by which to discriminate soil spatial variability, or to establish comparisons between soil management strategies.

Soil physical variables and capacitive indicators showed strong and significant correlations. Interesting relationships were observed for *Ks* with *PMACe*, *ACe* and *RFCe*. Remarkably, there were also strong inverse correlations between *RFCe* vs. *PMACe* and *ACe*. Similar to our findings, high negative correlations between relative field capacity and air capacity were observed in a previous study under different crop residue management (r within −0.949 and −0.956) and soil management strategies (r within −0.91 and −0.97) [32]. Strong positive correlations were also observed between macroporosity and air capacity. These outcomes confirm the strong correlation between *RFC* and *AC* and *PMAC* and *AC*. Decreasing *RFC* values at increasing *AC* were expected because both indicators depend on soil water content at saturation and at field capacity [32]. For the accuracy of the information brought by these indicators, in a previous study, *RFC* was considered as a reference indicator for soil quality assessment, and its optimal and critical ranges were used to define *AC* limits for agricultural soils [33].

Moran I spatial autocorrelation statistics provides useful information about the predisposition of the variables to be spatialized. In the present study, since the sample size was not excessively large, this could highly affect Moran outcomes. Therefore, values equal to, or larger than, 0.4 can be considered optimal. Generally, lower values of computed Moran statistics can be indicative of the incapability of catching the underlying spatial structure of the data and, in parallel, of the need for a more intensive sampling.

The experimental variograms calculated in this study can be considered reliable since a number of pairs for each distance class larger than the minimum required for an effective spatial analysis was ensured. Myers [14] suggested 25 pairs. In particular, the actual number of observed pairs ranged between 105 and 338.

From Table 3 it emerges that the spatial variability of all the considered variables, excluding *ACe*, are described by the exponential model; thus, this model was the best suited theoretical function to describe the spatial structure of the physical processes associated with the observed data. This result can be explained by two different perspectives. The first one is that of pure modeling, and the second is that of physical modeling. According to the first perspective, an exponential model represents the simplest case of the Matèrn model;

the latter is considered a part of what geostatisticians refer to as "the model" and the so-called *model-based geostatistics* [49] is based on the assumption that the Matèrn model can effectively mimic all the other models. By the second perspective, it should be recalled that the models reported in Figure 1 represent the average squared difference between couples of the observed values at given distances. Analyzing the functional form of the exponential model, it can be determined that values at the shortest distances are similar to each other (that is, for lag values (h) close to the origin), but very soon differences increase fast (Figure 1b). This is the usual empirical behavior of the considered variables; in fact, they are rather spatially heterogeneous due to their own physical nature, as highlighted in previous works [16,50]. The generalized attribution of the exponential model to *Ks* is confirmed by a large proportion of the scientific literature [51–54]. It should be noted that the range parameter assessed in each cited work always has a comparable order of magnitude.

As reported by several authors [25], the nugget-to-sill ratio has been computed as the ratio between the nugget semivariance and the total semivariance. This index, also called the Spatial Dependence Index (SDI), is largely employed to check the strength of the spatial structure [15,27], enabling the comparison of the relative size of the nugget effect of studied variables. In our study, a good overall spatial dependence was found for most of the investigated variables, except *BD*, *ACe* and *Ks*, which showed a moderate autocorrelation. These results resemble those found by Castellini et al. [32], for a different fine-textured soil in the same experimental area, where *Ks* had the weakest spatial dependence among the soil variables considered. Comparing the performances of *Ks* spatial modeling between the two studies, the poorest spatial structure observed in [32], with a nugget-to-sill ratio of 0.91, can be connected to the sample size (52 observations). In the present study, the larger sample size (72 observations) was able to grasp the underlying spatial processes, and this was reflected by the nugget-to-sill ratio (0.47). After the above comparison, we suggest a sample size larger than 70 observations for *Ks*, and overall to consider with caution the conclusions of the literature drawn from too small sample sizes. In recent studies, more intensive samplings (a number of observations larger than 90 and 200) have allowed for a significant improvement in the mapping accuracy of *Ks* [16,50].

Putting together the indications provided by the different indices computed, namely Moran I index, nugget-to-sill ratio, cross-validations outcomes and cross-correlation, it emerged that the sample size was probably nearly sufficient and needed to be increased for some of the variables, with particular regard to the hydrodynamic properties since, notoriously, *Ks* is characterized by a relatively high spatial variability [16,50]. The joint analysis of the abovementioned indices can help scholars and practitioners in setting an appropriate sample size for specific variables.

We want to highlight the positive role of cross-correlation statistics in the conducted analysis. The index is often neglected due to its complex formulation (Equation (2)). However, it enables a quantitative assessment of the behaviors emerging from the visual inspection of the prediction maps, thus making more objective their comparison [15,28]. Cross-correlations computed at lag (*h*) zero confirmed the expected strong relationship between the two capacitive indicators, air capacity and macroporosity, but also enabled us to highlight their spatial association with *Ks*. The range of spatial dependence was also coherent with the results of the variography. In addition, cross-correlation analysis disclosed the inverse spatial association between *Ks* and *BD* with the same range of spatial correlation.

As previously mentioned, repeated measurements performed over the same experimental unit may give rise to correlations that need to be considered in the statistical analysis [7]. However, classical analysis of variance and standard linear models assume independent errors [7,10]. Linear mixed effect models (LMMs), which quantify spatial correlation components and filter them from the total residual term of the model, may represent an appropriate strategy to be employed to improve the protection of statistical tests [9,55]. Previous studies have also shown that these models can enhance the understanding of factors affecting plant response, and are crucial in agronomic and environmental studies [55].

For these reasons, results obtained in this study also represent a first step towards the incorporation of information on the spatial structure of the investigated variables into more complex models (LMMs), with the aim of discerning the effects of compared treatments.

5. Conclusions

This study aimed to provide a set of suitable indicators, both estimated and directly measured in the field, which were useful in assessing the soil physical and hydraulic conditions. In addition, a set of statistical indicators, for gaining an integrated view of the spatial structure of the studied system, was proposed and applied. The results obtained represent a preliminary step for the inclusion of information on the spatial structure of soil hydraulic properties into linear mixed effects models considering residual autocorrelation.

A good overall spatial dependence was found for most of the investigated variables, except *BD*, *ACe* and *Ks*, which showed a moderate autocorrelation. In particular, *Ks* was confirmed to be characterized by a relatively high spatial variability, and thus, to require a more intensive spatial sampling. In this respect, machine leaning could provide a toolbox of methods advantageously applicable to predict this variable. In addition, the good cross-correlation observed in this study with some capacitive indicators seems to suggest the possibility to use these variables as covariates in predictive multivariate approaches.

The integrated use of spatial statistics demonstrated actual effectiveness in the interpretation of the spatial features of the single variables, as well as for couples. From a practical point of view, obtaining a large and spatially distributed set of data accounting for the physical and hydraulic properties of the soil can have positive implications for the rational management of water resources. However, although the applied methodology appears suitable to adequately investigate the spatial variability of soil physical and hydraulic properties at the plot/field scale, further development of this topic is necessary to consider more robust data sets, obtained, for example, from experimental measurements rather than modeling estimations or from coupling information derived from measured and estimated data.

Author Contributions: Conceptualization, S.P., E.B., M.C., F.F.M., A.M.S.; Methodology, E.B., A.M.S.; Formal analysis and data curation, E.B., A.M.S.; Investigation, S.P., M.C.; Writing—original draft preparation, E.B., A.M.S.; Writing—review and editing, S.P., E.B., M.C., F.F.M., A.M.S.; Funding acquisition, S.P., M.C., A.M.S. All authors have read and agreed to the published version of the manuscript.

Funding: This research received no external funding.

Data Availability Statement: Not applicable.

Acknowledgments: The work was also supported by PRIMA Fundation, call 2019-Section 1–GA n.1912 "Research-based participatory approaches for adopting Conservation Agriculture in the Mediterranean Area—CAMA" project. The authors would like to thank Alessandro Vittorio Vonella and Luisa Giglio for their valuable technical support. S. Popolizio developed this research for his Ph.D. activity.

Conflicts of Interest: The authors declare no conflict of interest.

References

1. Devine, S.; Markewitz, D.; Hendrix, P.; Coleman, D. Soil aggregates and associated organic matter under conventional tillage, no-tillage, and forest succession after three decades. *PLoS ONE* **2014**, *9*, e84988. [CrossRef] [PubMed]
2. Six, J.; Elliott, E.T.; Paustian, K. Aggregate and SOM dynamics under conventional and no-tillage systems. *Soil Sci. Soc. Am. J.* **1999**, *63*, 1350–1358. [CrossRef]
3. Blanco-Canqui, H.; Wienhold, B.J.; Jin, V.L.; Schmer, M.R. Long-term tillage impact on soil hydraulic properties. *Soil Tillage Res.* **2017**, *170*, 38–42. [CrossRef]
4. Ferrara, R.M.; Mazza, G.; Muschitiello, C.; Castellini, M.; Stellacci, A.M.; Navarro, A.; Lagomarsino, A.; Vitti, C.; Rossi, R.; Rana, G. Short-term effects of conversion to no-tillage on respiration and chemical-physical properties of the soil: A case study in a wheat cropping system in semi-dry environment. *Ital. J. Agrometeorol.* **2017**, *1*, 47–58. [CrossRef]

5. Stellacci, A.M.; Castellini, M.; Diacono, M.; Rossi, R.; Gattullo, C. Assessment of soil quality under different soil management strategies: Combined use of statistical approaches to select the most informative soil physico-chemical indicators. *Appl. Sci.* **2021**, *11*, 5099. [CrossRef]
6. Bevington, J.; Piragnolo, D.; Teatini, P.; Vellidis, G.; Morari, F. On the spatial variability of soil hydraulic properties in a Holocene coastal farmland. *Geoderma* **2016**, *262*, 294–305. [CrossRef]
7. Littell, R.C.; Milliken, G.A.; Stroup, W.W.; Wolfinger, R.D.; Schaberger, O. *SAS®System for Mixed Models*, 2nd ed.; SAS Institute Inc.: Cary, NC, USA, 2006.
8. Stellacci, A.M.; De Benedetto, D.; Leogrande, R.; Vitti, C.; Castellini, M.; Barca, E. Use of mixed effects models accounting for residual spatial correlation to analyze soil properties variation in a field irrigated with treated municipal wastewater. In Proceedings of the XLVII Conference of Italian Society for Agronomy, Marsala, Italy, 12–14 September 2018.
9. Ventrella, D.; Stellacci, A.M.; Castrignanò, A.; Charfeddine, M.; Castellini, M. Effects of crop residue management on winter durum wheat productivity in a long term experiment in Southern Italy. *Eur. J. Agron.* **2016**, *77*, 188–198. [CrossRef]
10. Hong, N.; White, J.G.; Gumpertz, M.L.; Weisz, R. Spatial analysis of precision agriculture treatments in randomized complete blocks: Guidelines for covariance model selection. *Agron. J.* **2005**, *97*, 1082–1096. [CrossRef]
11. Hu, X.; Spilke, J. Comparison of various spatial models for the analysis of hybrid trials. *N. Z. J. Agric. Res.* **2009**, *52*, 277–287. [CrossRef]
12. Journel, A.G.; Huijbregts, C.J. *Mining Geostatistics*; Academic Press: Waltham, MA, USA, 1978.
13. Webster, R.; Oliver, M.A. How large a sample is needed to estimate the regional variogram adequately? In *Geostatistics Tróia '92*; Springer: Berlin, Germany, 1993; pp. 155–166.
14. Myers, J.C. *Geostatistical Error Management: Quantifying Uncertainty for Environmental Sampling and Mapping*; John Wiley and Sons: Hoboken, NJ, USA, 1997.
15. De Benedetto, D.; Barca, E.; Castellini, M.; Popolizio, S.; Lacolla, G.; Stellacci, A.M. Prediction of soil organic carbon at field scale by Regression Kriging and Multivariate Adaptive Regression Splines using geophysical covariates. *Land* **2022**, *11*, 381. [CrossRef]
16. Usowicz, B.; Lipiec, J. Spatial variability of saturated hydraulic conductivity and its links with other soil properties at the regional scale. *Sci. Rep.* **2021**, *11*, 8293. [CrossRef]
17. Castellini, M.; Di Prima, S.; Moret-Fernández, D.; Lassabatère, L. Rapid and accurate measurement methods for determining soil hydraulic properties: A review. *J. Hydrol. Hydromech.* **2021**, *69*, 121–139. [CrossRef]
18. Haverkamp, R.; Arrúe, J.; Vandervaere, J.; Braud, I.; Boulet, G.; Laurent, J.; Taha, A.; Ross, P.; Angulo-Jaramillo, R. *Hydrological and Thermal Behaviour of the Vadose Zone in the Area of Barrax and Tomelloso (Spain): Experimental Study, Analysis and Modeling*; Project UE 1996; n. EV5C-CT 92, 00–90; European Union: Brussels, Belgium, 1996.
19. Lassabatère, L.; Angulo-Jaramillo, R.; Ugalde, J.M.S.; Cuenca, R.; Braud, I.; Haverkamp, R. Beerkan estimation of soil transfer parameters through infiltration experiments: BEST. *Soil Sci. Soc. Am. J.* **2006**, *70*, 521–532. [CrossRef]
20. Bagarello, V.; Di Prima, S.; Iovino, M.; Provenzano, G.; Sgroi, A. Testing different approaches to characterize Burundian soils by the BEST procedure. *Geoderma* **2011**, *162*, 141–150. [CrossRef]
21. Bagarello, V.; Di Prima, S.; Iovino, M.; Provenzano, G. Estimating field-saturated soil hydraulic conductivity by a simplified Beerkan infiltration experiment. *Hydrol. Process.* **2014**, *28*, 1095–1103. [CrossRef]
22. Barca, E.; Porcu, E.; Bruno, D.; Passarella, G. An automated decision support system for aided assessment of variogram models. *Environ. Model. Softw.* **2017**, *87*, 72–83. [CrossRef]
23. Bossong, C.R.; Karlinger, M.R.; Troutman, B.M.; Vecchia, A.V. *Overview and Technical and Practical Aspects for Use of Geostatistics in Hazardous-, Toxic-, and RadioactiveWaste-Site Investigations*; Water-Resources Investigations Report 98-4145; U.S. Geological Survey: Dencev, CO, USA, 1999. [CrossRef]
24. Bivand, R.; Altman, M.; Anselin, L.; Assunção, R.; Berke, O.; Bernat, A.; Blanchet, G. Package '*spdep*'. The Comprehensive R Archive Network. 2015. Available online: https://www.yumpu.com/en/document/view/24168126/package-spdep-the-comprehensive-r-archive-network (accessed on 28 September 2022).
25. Cambardella, C.A.; Elliott, E.T. Carbon and Nitrogen dynamics of soil organic matter fractions from cultivated grassland soils. *Soil Sci. Soc. Am. J.* **1994**, *58*, 123–130. [CrossRef]
26. Vieira, S.R.; Hatfield, T.L.; Nielsen, D.R.; Biggar, J.W. Geostatistical theory and application to variability of some agronomical properties. *Hilgardia* **1983**, *51*, 1–75. [CrossRef]
27. Pasini, M.P.B.; Dal'Col Lúcio, A.; Cargnelutti, A.F. Semivariogram models for estimating fig fly population density throughout the year. *Pesqui. Agropecu. Bras.* **2014**, *49*, 493–505. [CrossRef]
28. Barca, E.; Passarella, G. Spatial evaluation of the risk of groundwater quality degradation. A comparison between disjunctive kriging and geostatistical simulation. *Environ. Monit. Assess.* **2008**, *137*, 261–273. [CrossRef]
29. Barca, E.; De Benedetto, D.; Stellacci, A.M. Contribution of EMI and GPR proximal sensing data in soil water content assessment by using linear mixed effects models and geostatistical approaches. *Geoderma* **2019**, *343*, 280–293. [CrossRef]
30. UNESCO; FAO. *Bioclimatic Map of the Mediterranean Zone*; (NS162/III, 22A); UNESCO: Paris, France; FAO: Rome, Italy, 1963; p. 60.
31. Soil Survey Staff. *Soil Survey Field and Laboratory Methods Manual*; Soil Survey Investigations Report No. 51, Version 1.0; Burt, R., Ed.; U.S. Department of Agriculture, Natural Resources Conservation Service: Washington, DC, USA, 2009.

32. Castellini, M.; Stellacci, A.M.; Barca, E.; Iovino, M. Application of multivariate analysis techniques for selecting soil physical quality indicators: A case study in long-term field experiments in Apulia (Southern Italy). *Soil Sci. Soc. Am. J.* **2019**, *83*, 707–720. [CrossRef]
33. Castellini, M.; Stellacci, A.M.; Tomaiuolo, M.; Barca, E. Spatial variability of soil physical and hydraulic properties in a durum wheat field: An assessment by the BEST-Procedure. *Water* **2019**, *11*, 1434. [CrossRef]
34. Bagarello, V.; Di Prima, S.; Iovino, M. Comparing alternative algorithms to analyze the Beerkan infiltration experiment. *Soil Sci. Soc. Am. J.* **2014**, *78*, 724–736. [CrossRef]
35. Reynolds, W.D.; Drury, C.F.; Yang, X.M.; Fox, C.A.; Tan, C.S.; Zhang, T.Q. Land management effects on the near-surface physical quality of a clay loam soil. *Soil Tillage Res.* **2007**, *96*, 316–330. [CrossRef]
36. Reynolds, W.D.; Drury, C.F.; Tan, C.S.; Fox, C.A.; Yang, X.M. Use of indicators and pore volume-function characteristics to quantify soil physical quality. *Geoderma* **2009**, *152*, 252–263. [CrossRef]
37. Cavalcante, D.M.; Fonseca e Silva, A.P.; de Almeida, B.G.; Freire, F.J.; dos Santos Silva, T.H.; Silva Cavalcante, F.M. Physical soil quality indicators for environmental assessment and agricultural potential of Oxisols under different land uses in the Araripe Plateau, Brazil. *Soil. Tillage Res.* **2021**, *209*, 104951. [CrossRef]
38. FAO-ITPS 2020. *Protocol for the Assessment of Sustainable Soil Management*; FAO: Rome, Italy, 2020.
39. Carter, M.R. Temporal variability of soil macroporosity in a fine sandy loam under mouldboard ploughing and direct drilling. *Soil Tillage Res.* **1988**, *12*, 37–51. [CrossRef]
40. Drewry, J.J.; Cameron, K.C.; Buchan, G.D. Effect of simulated dairy cow treading on soil physical properties and ryegrass pasture yield. *N. Z. J. Agric. Res.* **2001**, *44*, 181–190. [CrossRef]
41. Drewry, J.J.; Paton, R.J. Soil physical quality under cattle grazing of a winter-fed brassica crop. *Aust. J. Soil Res.* **2005**, *43*, 525. [CrossRef]
42. Moran, P.A.P. Notes on continuous stochastic phenomena. *Biometrika* **1950**, *37*, 17–23. [CrossRef]
43. Rura, M.J.; Griffith, D.A. Spatial Statistics in SAS. In *Handbook of Applied Spatial Analysis*; Fischer, M., Getis, A., Eds.; Springer: Berlin/Heidelberg, Germany, 2010.
44. Mälicke, M.; Hassler, S.K.; Weiler, M.; Blume, T.; Zehe, E. Exploring hydrological similarity during soil moisture recession periods using time dependent variograms. *Hydrol. Earth Syst. Sci. Discuss.* **2018**, 1–25. [CrossRef]
45. SAS Institute Inc. *SAS/STAT Software Release 9.4*; SAS Institute Inc.: Cary, NC, USA, 2017.
46. Ribeiro, P.J., Jr.; Diggle, P.J. R: A package for geostatistical analysis. *R News* **2001**, *1*, 14–18.
47. Isaaks, E.H.; Srivastava, R.M. *An Introduction to Applied Geostatistics*; Oxford University Press: New York, NY, USA, 1989.
48. Stein, A.; Brouwer, J.; Bouma, J. Methods for comparing spatial variability patterns of millet yield and soil data. *Soil Sci. Soc. Am. J.* **1997**, *61*, 861–870. [CrossRef]
49. Diggle, P.J.; Ribeiro, P.J.; Christensen, O.F. An introduction to model-based geostatistics. In *Spatial Statistics and Computational Methods*; Springer: New York, NY, USA, 2003; pp. 43–86.
50. Gupta, N.; Rudra, R.P.; Parkin, G. Analysis of spatial variability of hydraulic conductivity at field scale. *Can. Biosyst. Eng.* **2006**, *48*, 55–62.
51. Gallichand, J.; Prasher, S.O.; Broughton, R.S.; Marcotte, D. Kriging of hydraulic conductivity for subsurface drainage design. *J. Irrig. Drain. Eng.* **1991**, *117*, 667–681. [CrossRef]
52. Motaghian, H.R.; Mohammadi, J. Spatial estimation of saturated hydraulic conductivity from terrain attributes using regression, kriging, and artificial neural networks. *Pedosphere* **2011**, *21*, 170–177. [CrossRef]
53. Troisi, S.; Fallico, C.; Straface, S.; Migliari, E. Application of kriging with external drift to estimate hydraulic conductivity from electrical-resistivity data in unconsolidated deposits near Montalto Uffugo, Italy. *Hydrogeol. J.* **2000**, *8*, 356–367. [CrossRef]
54. Ghosh, B.; Pekkat, S. An appraisal on the interpolation methods used for predicting spatial variability of field hydraulic conductivity. *Water Resour. Manag.* **2019**, *33*, 2175–2190. [CrossRef]
55. Rodrigues, M.S.; Corà, J.E.; Castrignanò, A.; Mueller, T.G.; Rienzi, E. A spatial and temporal prediction model of corn grain yield as a function of soil attributes. *Agron. J.* **2013**, *105*, 1878–1886. [CrossRef]